

Accurate Online Posterior Alignments for Principled Lexically-Constrained Decoding

Anonymous ACL submission

Abstract

Online alignment in machine translation refers to the task of aligning a target word to a source word when the target sequence has only been partially decoded. Good online alignments facilitate important applications such as lexically constrained translation where user-defined dictionaries are used to inject lexical constraints into the translation model. We propose a novel posterior alignment technique that is truly online in its execution and superior in terms of alignment error rates compared to existing methods. Our proposed inference technique jointly considers alignment and token probabilities in a principled manner and can be seamlessly integrated within existing constrained beam-search decoding algorithms. On five language pairs, including two distant language pairs, we achieve consistent drop in alignment error rates. When deployed on seven lexically constrained translation tasks, we achieve significant improvements in BLEU specifically around the constrained positions.

1 Introduction

Online alignment seeks to align a target word to a source word at the decoding step when the word is output in an auto-regressive neural translation model (Kalchbrenner and Blunsom, 2013; Cho et al., 2014; Sutskever et al., 2014). This is unlike the more popular offline alignment task that uses the entire target sentence (Och and Ney, 2003; Jalili Sabet et al., 2020; Dou and Neubig, 2021). An important application of online alignment is lexically constrained translation which allows injection of domain-specific terminology and other phrasal constraints during decoding (Hasler et al., 2018; Hokamp and Liu, 2017; Alkhoul et al., 2018; Crego et al., 2016). Other applications include preservation of markups between the source and target (Müller, 2017), and supporting source word edits in summarization (Shen et al., 2019). These

applications need to infer the specific source token which aligns with output token. Thus, alignment and translation is to be done simultaneously.

Existing online alignment methods can be categorized into Prior and Posterior alignment methods. Prior alignment methods (Garg et al., 2019; Song et al., 2020) extract alignment based on the attention at time step t when outputting token y_t . The attention probabilities at time-step t are conditioned on tokens output before time t . Thus, the alignment is estimated *prior* to observing y_t . Naturally, the quality of alignment can be improved if we condition on the target token y_t (Shankar and Sarawagi, 2019). This motivated Chen et al. (2020) to propose a posterior alignment method where alignment is calculated from the attention probabilities at the next decoder step $t + 1$. While alignment quality improved as a result, their method is not truly online since it does not generate alignment *synchronously* with the token. The delay of one step makes it difficult and cumbersome to incorporate terminology constraints during beam decoding.

We propose a truly online posterior alignment method that provides higher alignment accuracy than existing online methods, while also being synchronous. Because of that we can easily integrate posterior alignment to improve lexicon-constrained translation in state of the art constrained beam-search algorithms such as VDBA (Hu et al., 2019). Our method (Align-VDBA) presents a significant departure from existing papers on alignment-guided constrained translation (Chen et al., 2020; Song et al., 2020) that employ a greedy algorithm with poor constraint satisfaction rate (CSR). For example, on a ja→en their CSR is 20 points lower than ours. Moreover, the latter does not benefit from larger beam sizes unlike VDBA-based methods that significantly improve with larger beam widths. Compared to Chen et al. (2020), our method improves average overall BLEU scores by 1.2 points and average BLEU scores around the

constrained span by up to 9 points. In the evaluations performed in these earlier work, VDBA was not allocated the slightly higher beam size needed to pro-actively enforce constraints without compromising BLEU. Compared to Hu et al. (2019) (VDBA), this paper’s contributions include online alignments and their use in more fluent constraint placement and efficient allocation of beams.

Contributions

- A truly online posterior alignment method that integrates into existing NMT systems via a trainable light-weight module.
- Higher online alignment accuracy on five language pairs including two distant language pairs where we improve over the best existing in seven out of ten translation models.
- Principled method of modifying VDBA to incorporate posterior alignment probabilities in lexically-constrained decoding. VDBA enforces constraints ignoring source alignments, our change (Align-VDBA), leads to more fluent constraint placement and significant BLEU increase particularly for smaller beams.
- Establishing that VDBA-based pro-active constrained inference should be preferred over prevailing greedy alignment-guided inference (Chen et al., 2021; Song et al., 2020). Further, VDBA and our Align-VDBA inference with beam size 10 provide 1.2 BLEU increase over these methods with the same beam size.

2 Posterior Online Alignment

Given a sentence $\mathbf{x} = x_1, \dots, x_S$ in the source language and a sentence $\mathbf{y} = y_1, \dots, y_T$ in the target language, an alignment \mathcal{A} between the word strings is a subset of the Cartesian product of the word positions (Brown et al., 1993; Och and Ney, 2003): $\mathcal{A} \subseteq \{(s, t) : s = 1, \dots, S; t = 1, \dots, T\}$ such that the aligned words can be considered translations of each other. An online alignment at time-step t commits on alignment of the t^{th} output token conditioned only on \mathbf{x} and $\mathbf{y}_{<t} = y_1, y_2, \dots, y_{t-1}$. Additionally, if token y_t is also available we call it a posterior online alignment. We seek to embed online alignment with existing NMT systems. We will first briefly describe the architecture of state of the art NMT systems. We will then elaborate on how alignments are computed from attention distributions in prior work and highlight some limitations, before describing our proposed approach.

2.1 Background

Transformers (Vaswani et al., 2017) adopt the popular encoder-decoder paradigm used for sequence-to-sequence modeling (Cho et al., 2014; Sutskever et al., 2014; Bahdanau et al., 2015). The encoder and decoder are both multi-layered networks with each layer consisting of a multi-headed self-attention and a feedforward module. The decoder uses multi-headed attention to encoder states. We elaborate on this mechanism next since it plays an important role in alignments.

2.1.1 Decoder-Encoder Attention in NMTs

The encoder transforms the S input tokens into a sequence of token representations $\mathbf{H} \in \mathbb{R}^{S \times d}$. Each decoder layer (indexed by $\ell \in \{1, \dots, L\}$) computes multi-head attention over \mathbf{H} by aggregating outputs from a set of η independent attention heads. The attention output from a single head $n \in \{1, \dots, \eta\}$ in decoder layer ℓ is computed as follows. Let the output of the self-attention sub-layer in decoder layer ℓ at the t^{th} target token be denoted as \mathbf{g}_t^ℓ . Using three projection matrices $\mathbf{W}_Q^{\ell,n}, \mathbf{W}_V^{\ell,n}, \mathbf{W}_K^{\ell,n} \in \mathbb{R}^{d \times d_n}$, the query vector $\mathbf{q}_t^{\ell,n} \in \mathbb{R}^{1 \times d_n}$ and key and value matrices, $\mathbf{K}^{\ell,n} \in \mathbb{R}^{S \times d_n}$ and $\mathbf{V}^{\ell,n} \in \mathbb{R}^{S \times d_n}$, are computed using the following projections: $\mathbf{q}_t^{\ell,n} = \mathbf{g}_t^\ell \mathbf{W}_Q^{\ell,n}$, $\mathbf{K}^{\ell,n} = \mathbf{H} \mathbf{W}_K^{\ell,n}$, and $\mathbf{V}^{\ell,n} = \mathbf{H} \mathbf{W}_V^{\ell,n}$.¹ These are used to calculate the attention output from head n , $\mathbf{Z}_t^{\ell,n} = P(\mathbf{a}_t^{\ell,n} | \mathbf{x}, \mathbf{y}_{<t}) \mathbf{V}^{\ell,n}$, where:

$$P(\mathbf{a}_t^{\ell,n} | \mathbf{x}, \mathbf{y}_{<t}) = \text{softmax} \left(\frac{\mathbf{q}_t^{\ell,n} (\mathbf{K}^{\ell,n})^\top}{\sqrt{d}} \right) \quad (1)$$

For brevity, the conditioning on $\mathbf{x}, \mathbf{y}_{<t}$ is dropped and $P(\mathbf{a}_t^{\ell,n})$ is used to refer to $P(\mathbf{a}_t^{\ell,n} | \mathbf{x}, \mathbf{y}_{<t})$ in the following sections.

Finally, the multi-head attention output is given by $[\mathbf{Z}_t^{\ell,1}, \dots, \mathbf{Z}_t^{\ell,\eta}] \mathbf{W}^O$ where $[\]$ denotes the column-wise concatenation of matrices and $\mathbf{W}^O \in \mathbb{R}^{d \times d}$ is an output projection matrix.

2.1.2 Alignments from Attention

Several prior work have proposed to extract word alignments from the above attention probabilities. For example Garg et al. (2019) propose a simple method called NAIVEATT that aligns a source word to the t^{th} target token using

¹ d_n is typically set to $\frac{d}{\eta}$ so that a multi-head attention layer does not introduce more parameters compared to a single head attention layer.

175 $\operatorname{argmax}_j \frac{1}{\eta} \sum_{n=1}^{\eta} P(a_{t,j}^{\ell,n} | \mathbf{x}, \mathbf{y}_{<t})$ where j indexes

176 the source tokens. In NAIVEATT, we note that the
 177 attention probabilities $P(a_{t,j}^{\ell,n} | \mathbf{x}, \mathbf{y}_{<t})$ at decoding
 178 step t are not conditioned on the current output to-
 179 ken y_t . Alignment quality would benefit from condi-
 180 tioning on y_t as well. This observation prompted
 181 [Chen et al. \(2020\)](#) to extract alignment of token y_t
 182 using attention $P(a_{t,j}^{\ell,n} | \mathbf{x}, \mathbf{y}_{<t})$ computed at time
 183 step $t + 1$. The asynchronicity inherent to this shift-
 184 by-one approach (SHIFTATT) makes it difficult
 185 and more computationally expensive to incorporate
 186 lexical constraints during beam decoding.

2.2 Our Proposed Method: POSTALN

187 We propose POSTALN that produces posterior
 188 alignments synchronously with the output tokens,
 189 while being more computationally efficient com-
 190 pared to previous approaches like SHIFTATT. We
 191 incorporate a lightweight alignment module to con-
 192 vert prior attention to posterior alignments in the
 193 same decoding step as the output. Figure 1 illus-
 194 trates how this alignment module fits within the
 195 standard Transformer architecture.

197 The alignment module is placed at the penulti-
 198 mate decoder layer $\ell = L - 1$ and takes as input
 199 1) the encoder output \mathbf{H} , 2) the output of the self-
 200 attention sub-layer of decoder layer ℓ , \mathbf{g}_t^ℓ and, 3)
 201 the embedding of the decoded token $\mathbf{e}(y_t)$. Like
 202 in standard attention it projects \mathbf{H} to obtain a key
 203 matrix, but to obtain the query matrix it uses both
 204 decoder state \mathbf{g}_t^ℓ (that summarizes $\mathbf{y}_{<t}$) and $\mathbf{e}(y_t)$
 205 to compute the posterior alignment $P(\mathbf{a}_t^{\text{post}})$ as:

$$206 \quad P(\mathbf{a}_t^{\text{post}}) = \frac{1}{\eta} \sum_{n=1}^{\eta} \operatorname{softmax} \left(\frac{\mathbf{q}_{t,\text{post}}^n (\mathbf{K}_{\text{post}}^n)^\top}{\sqrt{d}} \right),$$

$$207 \quad \mathbf{q}_{t,\text{post}}^n = [\mathbf{g}_t^\ell, \mathbf{e}(y_t)] \mathbf{W}_{Q,\text{post}}^n, \quad \mathbf{K}_{\text{post}}^n = \mathbf{H} \mathbf{W}_{K,\text{post}}^n$$

208 Here $\mathbf{W}_{Q,\text{post}}^n \in \mathbb{R}^{2d \times d_n}$ and $\mathbf{W}_{K,\text{post}}^n \in \mathbb{R}^{d \times d_n}$.

209 This computation is synchronous with produc-
 210 ing the target token y_t , thus making it compatible
 211 with beam search decoding (as elaborated further
 212 in Section 3). It also accrues minimal computa-
 213 tional overhead since $P(\mathbf{a}_t^{\text{post}})$ is defined using \mathbf{H}
 214 and \mathbf{g}_t^{L-1} , that are both already cached during a
 215 standard decoding pass. Note that if the query vec-
 216 tor $\mathbf{q}_{t,\text{post}}^n$ is computed using only \mathbf{g}_t^{L-1} , without
 217 concatenating $\mathbf{e}(y_t)$, then we get prior alignments
 218 that we refer to as PRIORATT. In our experiments,
 219 we explicitly compare PRIORATT with POSTALN
 220 to show the benefits of using y_t in deriving align-

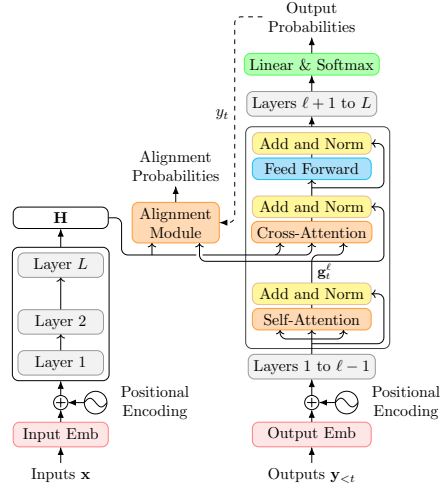


Figure 1: Our alignment module is an encoder-
 decoder attention sub-layer, similar to the existing
 cross-attention sub-layer. It takes as inputs the encoder
 output \mathbf{H} as the key, and the concatenation of the output
 of the previous self-attention layer \mathbf{g}_t^ℓ and the currently
 decoded token y_t as the query, and outputs posterior
 alignment probabilities $\mathbf{a}_t^{\text{post}}$.

221 ments while keeping the rest of the architecture
 222 intact.

223 **Training** Our posterior alignment sub-layer is
 224 trained using alignment supervision, while freez-
 225 ing the rest of the translation model parameters.
 226 Specifically, we train a total of $3d^2$ additional pa-
 227 rameters across the matrices $\mathbf{W}_{K,\text{post}}^n$ and $\mathbf{W}_{Q,\text{post}}^n$.
 228 Since gold alignments are very tedious and expen-
 229 sive to create for large training datasets, alignment
 230 labels are typically obtained using existing tech-
 231 niques. We use bidirectional symmetrized SHIF-
 232 TATT alignments, denoted by $S_{i,j}$ that refers to an
 233 alignment between the i^{th} target word and the j^{th}
 234 source word, as reference labels to train our align-
 235 ment sub-layer. Then the objective (following [Garg
 et al. \(2019\)](#)) can be defined as:
 236

$$237 \quad \max_{\mathbf{W}_{Q,\text{post}}^n, \mathbf{W}_{K,\text{post}}^n} \frac{1}{T} \sum_{i=1}^T \sum_{j=1}^S S_{i,j} \log \left(P(a_{i,j}^{\text{post}} | \mathbf{x}, \mathbf{y}_{\leq i}) \right)$$

238 Next, we demonstrate the role of posterior online
 239 alignments on an important downstream task.

3 Lexicon Constrained Translation

240 In the lexicon constrained translation task, for
 241 each to-be-translated sentence \mathbf{x} , we are given a
 242 set of source text spans and the corresponding
 243 target tokens in the translation. A constraint \mathcal{C}_j
 244 comprises a pair $(\mathcal{C}_j^x, \mathcal{C}_j^y)$ where $\mathcal{C}_j^x = (p_j, p_j +$
 245

$1 \dots, p_j + \ell_j$) indicates input token positions, and $\mathcal{C}_j^y = (y_1^j, y_2^j \dots, y_{m_j}^j)$ denote target tokens that are translations of the input tokens $x_{p_j} \dots x_{p_j + \ell_j}$. For the output tokens we do not know their positions in the target sentence. The different constraints are non-overlapping and each is expected to be used exactly once. The goal is to translate the given sentence \mathbf{x} and satisfy as many constraints in $\mathcal{C} = \bigcup_j \mathcal{C}_j$ as possible while ensuring fluent and correct translations. Since the constraints do not specify target token position, it is natural to use online alignments to guide when a particular constraint is to be enforced.

3.1 Background: Constrained Decoding

Existing inference algorithms for incorporating lexicon constraints differ in how pro-actively they enforce the constraints. A passive method is used in Song et al. (2020) where constraints are enforced only when the prior alignment is at a constrained source span. Specifically, if at decoding step t , $i = \operatorname{argmax}_{i'} P(a_{t,i'})$ is present in some constraint \mathcal{C}_j^x , the output token is fixed to the first token y_1^j from \mathcal{C}_j^y . Otherwise, the decoding proceeds as usual. Also, if the translation of a constraint \mathcal{C}_j has started, the same is completed (y_2^j through $y_{m_j}^j$) for the next $m_j - 1$ decoding steps before resuming unconstrained beam search. The pseudocode for this method is provided in Appendix G.

For the posterior alignment methods of Chen et al. (2020) this leads to a rather cumbersome inference (Chen et al., 2021). First, at step t they predict a token \hat{y}_t , then start decoding step $t + 1$ with \hat{y}_t as input to compute the posterior alignment from attention at step $t + 1$. If the maximum alignment is to the constrained source span \mathcal{C}_j^x they *revise* the output token to be y_1^j from \mathcal{C}_j^y , but the output score for further beam-search continues to be of \hat{y}_t . In this process both the posterior alignment and token probabilities are misrepresented since they are both based on \hat{y}_t instead of the finally output token y_1^j . The decoding step at $t + 1$ needs to be restarted after the revision. The overall algorithm continues to be normal beam-search, which implies that the constraints are not enforced pro-actively.

Many prior methods have proposed more proactive methods of enforcing constraints, including the Grid Beam Search (GBA, Hokamp and Liu (2017)), Dynamic Beam Allocation (DBA, Post and Vilar (2018)) and Vectorized Dynamic Beam Allocation (VDBA, Hu et al. (2019)). The latest

of these, VDBA, is efficient and available in public NMT systems (Ott et al., 2019; Hieber et al., 2020). Here multiple *banks*, each corresponding to a particular number of completed constraints, are maintained. At each decoding step, a hypothesis can either start a new constraint and move to a new bank or continue in the same bank (either by not starting a constraint or progressing on a constraint mid-completion). This allows them to achieve near 100% enforcement. However, VDBA enforces the constraints by considering only the target tokens of the lexicon and totally ignores the alignment of these tokens to the source span. This could lead to constraints being placed at unnatural locations leading to loss of fluency. Examples appears in Table 4 where we find that VDBA just attaches the constrained tokens at the end of the sentence.

3.2 Our Proposal: Align-VDBA

We modify VDBA with alignment probabilities to better guide constraint placement. The score of a constrained token is now the joint probability of the token, and the probability of the token being aligned with the corresponding constrained source span. Formally, if the current token y_t is a part of the j^{th} constraint *i.e.* $y_t \in \mathcal{C}_j^y$, the generation probability of y_t , $P(y_t | \mathbf{x}, \mathbf{y}_{<t})$ is scaled by multiplying with the alignment probabilities of y_t with \mathcal{C}_j^x , the source span for constraint i . Thus, the updated probability is given by:

$$\underbrace{P(y_t, \mathcal{C}_j^x | \mathbf{x}, \mathbf{y}_{<t})}_{\text{Joint Prob}} = \underbrace{P(y_t | \mathbf{x}, \mathbf{y}_{<t})}_{\text{Token Prob}} \underbrace{\sum_{r \in \mathcal{C}_j^x} P(a_{t,r}^{\text{post}} | \mathbf{x}, \mathbf{y}_{\leq t})}_{\text{Src Align. Prob.}} \quad (2)$$

$P(y_t, \mathcal{C}_j^x | \mathbf{x}, \mathbf{y}_{<t})$ denotes the joint probability of outputting the constrained token and the alignment being on the corresponding source span. Since the supervision for the alignment probabilities was noisy, we found it useful to recalibrate the alignment distribution using a temperature scale T , so that the recalibrated probability is $\propto \Pr(a_{t,r}^{\text{post}} | \mathbf{x}, \mathbf{y}_{\leq t})^{\frac{1}{T}}$. We used $T = 2$ *i.e.*, square-root of the alignment probability.

Align-VDBA uses posterior alignment probabilities to also improve the efficiency of DBA. Currently, DBA attempts beam allocation for each unmet constraint since it has no way to discriminate. In Align-VDBA we allocate only when the alignment probability is greater than a threshold. When the beam size is small (say 5) this yields higher accuracy due to more efficient beam utilization.

Algorithm 1 Align-VDBA: Modifications to DBA shown in blue. (Adapted from Post and Vilar (2018))

```
1: Inputs beam:  $K$  hypothesis in beam, scores:  $K \times |V_T|$  matrix of scores where scores[ $k, y$ ] denotes the score of  $k^{\text{th}}$ 
   hypothesis extended with token  $y$  at this step, constraints:  $\{(C_j^x, C_j^y)\}$ 
2: candidates  $\leftarrow [(k, y, \text{scores}[k, y], \text{beam}[k].\text{constraints.add}(y)) \text{ for } k, y \text{ in ARGMAX\_K}(\text{scores})]$ 
3: for  $1 \leq k \leq K$  do ▷ Go over current beam
4:   for all  $y \in V_T$  that are unmet constraints for beam[ $k$ ] do ▷ Expand new constraints
5:     alignProb  $\leftarrow \Sigma_{\text{constraint\_xs}(y)} \text{POSTALN}(k, y)$  ▷ Modification in blue (Eqn (2))
6:     if alignProb > threshold (= 0.1) then
7:       candidates.append( ( $k, y, \text{scores}[k, y] \times \text{alignProb}$ ), beam[ $k$ ].constraints.add( $y$ ) )
8:       candidates.append( ( $k, y, \text{scores}[k, y]$ , beam[ $k$ ].constraints.add( $y$ ) ) ) ▷ Original DBA Alg.
9:    $w = \text{ARGMAX}(\text{scores}[k, :])$ 
10:  candidates.append( ( $k, w, \text{scores}[k, w]$ , beam[ $k$ ].constraints.add( $w$ ) ) ) ▷ Best single word
11: newBeam  $\leftarrow \text{ALLOCATE}(\text{candidates}, K)$ 
```

343 We present the pseudocode of our modification
344 (steps 5, 6 and 7, in blue) to DBA in Algorithm 1.
345 Other details of the algorithm including the han-
346 dling of constraints and the allocation steps (step
347 11) are involved and we refer the reader to Post
348 and Vilar (2018) and Hu et al. (2019) to understand
349 these details. The point of this code is to show that
350 our proposed posterior alignment method can be
351 easily incorporated into these algorithms so as to
352 provide a more principled scoring of constrained
353 hypothesis in a beam than the ad hoc revision-based
354 method of Chen et al. (2021). Additionally, pos-
355 terior alignments lead to better placement of con-
356 straints than in the original VDBA algorithm.

357 4 Experiments

358 We first compare our proposed posterior online
359 alignment method on quality of alignment against
360 existing methods in Section 4.2, and in Section 4.3,
361 we demonstrate the impact of the improved align-
362 ment on the lexicon-constrained translation task.

363 4.1 Setup

364 We deploy the fairseq toolkit (Ott et al., 2019)
365 and use transformer_iwslt_de_en pre-
366 configured model for all our experiments. Other
367 configuration parameters include: Adam optimizer
368 with $\beta_1 = 0.9$, $\beta_2 = 0.98$, a learning rate of $5e-4$
369 with 4000 warm-up steps, an inverse square root
370 schedule, weight decay of $1e-4$, label smoothing
371 of 0.1, 0.3 probability dropout and a batch size of
372 4500 tokens. The transformer models are trained
373 for 50,000 iterations. Then, the alignment module
374 is trained for 10,000 iterations, keeping the other
375 model parameters fixed. A joint byte pair encoding
376 (BPE) is learned for the source and the target lan-
377 guages with 10k merge operation (Sennrich et al.,
378 2016) using subword-nmt.

379 All experiments were done on a single 11GB

	de-en	en-fr	ro-en	en-hi	ja-en
Training	1.9M	1.1M	0.5M	1.6M	0.3M
Validation	994	1000	999	25	1166
Test	508	447	248	140	1235

Table 1: Number of sentence pairs for the five datasets used. Note that gold alignments are available only for a handful of sentence pairs in the test set.

Nvidia GeForce RTX 2080 Ti GPU on a machine 380
with 64 core Intel Xeon CPU and 755 GB memory. 381
The vanilla Transformer models take between 15 382
to 20 hours to train for different datasets. Starting 383
from the alignments extracted from these models, 384
the POSTALN alignment module trains in about 3 385
to 6 hours depending on the dataset. 386

387 4.2 Alignment Task

388 We evaluate online alignments on ten translation 388
tasks spanning five language pairs. Three of these 389
are popular in alignment papers (Zenkel et al., 390
2019): German-English (de-en), English-French 391
(en-fr), Romanian-English (ro-en). These are all 392
European languages that follow the same subject- 393
verb-object (SVO) ordering. We also present re- 394
sults on two distant language pairs, English-Hindi 395
(en-hi) and English-Japanese (ja-en), that follow a 396
SOV word order which is different from the SVO 397
word order of English. Data statistics are shown in 398
Table 1 and details are in Appendix C. 399

Evaluation Method: For evaluating alignment 400
performance, it is necessary that the target sentence 401
is exactly the same as for which the gold alignments 402
are provided. Thus, for the alignment experiments, 403
we force the output token to be from the gold tar- 404
get and only infer the alignment. We then report 405
the Alignment Error Rate (AER) (Och and Ney, 406
2000) between the gold alignments and the pre- 407
dicted alignments for different methods. Though 408

Method	Delay	de-en		en-fr		ro-en		en-hi		ja-en	
		de→en	en→de	en→fr	fr→en	ro→en	en→ro	en→hi	hi→en	ja→en	en→ja
Statistical Methods (Not Online)											
GIZA++ (Och and Ney, 2003)	End	18.9	19.7	7.3	7.0	27.6	28.3	35.9	36.4	41.8	39.0
FastAlign (Dyer et al., 2013)	End	28.4	32.0	16.4	15.9	33.8	35.5	-	-	-	-
No Alignment Training											
NAIVEATT (Garg et al., 2019)	0	32.4	40.0	24.0	31.2	37.3	33.2	49.1	53.8	62.2	63.5
SHIFTATT (Chen et al., 2020)	+1	20.0	22.9	14.7	20.4	26.9	27.4	35.3	38.6	53.6	48.6
With Alignment Training											
PRIORATT	0	23.4	25.8	14.0	16.6	29.3	27.2	36.4	35.1	52.7	50.9
SHIFTAET (Chen et al., 2020)	+1	15.8	19.5	10.3	10.4	22.4	23.7	29.3	29.3	42.5	41.9
POSTALN [Ours]	0	15.5	19.5	9.9	10.4	21.8	23.2	28.7	28.9	41.2	42.2

Table 2: AER for de-en, en-fr, ro-en, en-hi, ja-en language pairs. “Delay” indicates the decoding step at which the alignment of the target token is available. NAIVEATT, PRIORATT and POSTALN are truly online and output alignment at the same time step (delay=0), while SHIFTATT and SHIFTAET output one decoding step later.

our focus is online alignment, for comparison to previous works, we also report results on bidirectional symmetrized alignments in Appendix D.

Methods compared: We compare our method with both existing statistical alignment models, namely GIZA++ (Och and Ney, 2003) and FastAlign (Dyer et al., 2013), and recent Transformer-based alignment methods of Garg et al. (2019) (NAIVEATT) and Chen et al. (2020) (SHIFTATT and SHIFTAET). Chen et al. (2020) also propose a variant of SHIFTATT called SHIFTAET that delays computations by one time-step as in SHIFTATT, and additionally includes a learned attention sub-layer to compute alignment probabilities. We also present results on PRIORATT which is similar to POSTALN but does not use y_t .

Results: The alignment results are shown in Table 2. First, AERs using statistical methods FastAlign and GIZA++ are shown. Here, for fair comparison, the IBM models used by GIZA++ are trained on the same sub-word units as the Transformer models and sub-word alignments are converted to word level alignments for AER calculations. (GIZA++ has remained a state-of-the-art alignment technique and continues to be compared against.) Next, we present alignment results for two vanilla Transformer models - NAIVEATT and SHIFTATT - that do not train a separate alignment module. The high AER of NAIVEATT shows that attention-as-is is very distant from alignment but posterior attention is closer to alignments than prior. Next we look at methods that train alignment-specific parameters: PRIORATT, a prior attention method; SHIFTAET and POSTALN, both posterior alignment methods. We observe that with training even PRIORATT has surpassed non-trained posterior. The posterior attention methods outperform the prior attention

methods by a large margin, with an improvement of 4.0 to 8.0 points. Within each group, the methods with a trained alignment module outperform the ones without by a huge margin. POSTALN performs better or matches the performance of SHIFTAET (achieving the lowest AER in nine out of ten cases in Table 2) while avoiding the one-step delay in alignment generation. Even on the distant languages, POSTALN achieves significant reductions in error. For ja→en, we achieve a 1.3 AER reduction compared to SHIFTAET which is not a truly online method. Figure 2 shows an example to illustrate the superior alignments of POSTALN compared to NAIVEATT and PRIORATT.

4.3 Impact of POSTALN on Lexicon-Constrained Translation

We next depict the impact of improved AERs from our posterior alignment method on a downstream lexicon-constrained translation task. Following previous work (Hokamp and Liu, 2017; Post and Vilar, 2018; Song et al., 2020; Chen et al., 2020, 2021), we extract constraints using the gold alignments and gold translations. Up to three constraints of up to three words each are used for each sentence. Spans correctly translated by a greedy decoding are not selected as constraints.

Metrics: Following prior work (Song et al., 2020): we report BLEU (Papineni et al., 2002), time to translate all test sentences, and Constraint Satisfaction Rate (CSR). and However, since it is trivial to get 100% CSR by always copying, we report another metric to evaluate the appropriateness of constraint placement: We call this measure BLEU-C and compute it as the BLEU of the constraint (when satisfied) and a window of three words around it. All numbers are averages over five different sets of

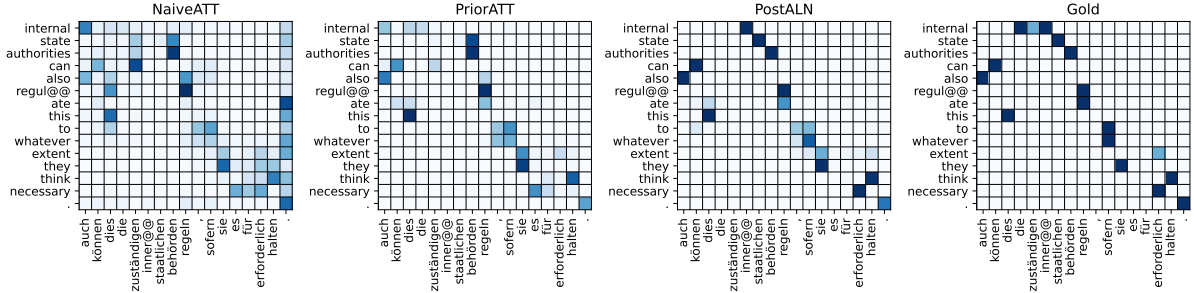


Figure 2: Alignments for de→en by NAIVEATT, PRIORATT, and POSTALN. Note that POSTALN is most similar to Gold alignments in the last column.

Method	de→en				en→fr				ro→en				en→hi				ja→en			
	BLEU-C	CSR	BLEU	Time	BLEU-C	CSR	BLEU	Time	BLEU-C	CSR	BLEU	Time	BLEU-C	CSR	BLEU	Time	BLEU-C	CSR	BLEU	Time
No constraints	0.0	4.6	32.9	87	0.0	8.7	34.8	64	0.0	8.8	33.4	47	0.0	6.3	19.7	21	0.0	8.8	18.9	237
NAIVEATT	28.7	86.1	36.6	147	36.5	88.0	38.3	93	33.3	92.3	36.5	99	22.5	88.4	23.6	27	15.1	75.9	20.2	315
PRIORATT	35.0	92.8	37.6	159	42.1	94.4	38.9	97	36.0	91.2	37.2	100	27.2	91.5	24.4	28	16.7	79.7	20.4	326
SHIFTATT	41.0	96.6	38.7	443	45.0	93.5	38.7	239	39.2	94.2	37.4	241	23.2	78.7	21.9	58	15.2	72.7	19.3	567
SHIFTAET	43.1	97.5	39.1	458	46.6	94.3	39.0	235	40.8	94.4	37.6	263	24.3	80.2	22.0	62	18.1	75.9	19.7	596
POSTALN	42.7	97.2	39.0	399	46.3	94.1	38.7	218	40.0	93.5	37.4	226	23.8	79.0	22.0	47	18.2	75.7	19.7	460
VDBA	44.5	98.9	38.5	293	51.9	98.5	39.5	160	43.1	99.1	37.9	165	29.8	92.3	24.5	49	24.3	95.6	21.6	494
Align-VDBA	44.5	98.6	38.6	357	52.9	98.4	39.7	189	44.1	98.9	38.1	203	30.5	91.5	24.7	70	25.1	95.5	21.8	630

Table 3: Constrained translation results showing BLEU-C, CSR (Constraint Satisfaction Rate), BLEU scores and total decoding time (in seconds) for the test set. Align-VDBA has the highest BLEU-C on all datasets.

randomly sampled constraint sets. The beam size is set to ten by default; results for other beam sizes appear in Appendix E.

Methods Compared: First we compare all the alignment methods presented in Section 4.2 on the constrained translation task using the alignment based token-replacement algorithm of Song et al. (2020) described in Section 3.1. Next, we present a comparison between VDBA (Hu et al., 2019) and our modification Align-VDBA.

Results: Table 3 shows that VDBA and our Align-VDBA that pro-actively enforce constraints have a much higher CSR and BLEU-C compared to the other lazy constraint enforcement methods. For example, for ja→en greedy methods can only achieve a CSR of 76% compared to 96% of the VDBA-based methods. In terms of overall BLEU too these methods provide an average increase in BLEU of 1.2 and an average increase in BLEU-C of 5 points. On average, Align-VDBA has a 0.7 point greater BLEU-C compared to VDBA. It also has a greater BLEU than VDBA on all the five datasets. In Table 9 of Appendix we show that for smaller beam-size of 5, the gap between Align-VDBA and VDBA is even larger (2.1 points greater BLEU-C and 0.4 points greater BLEU). Table 4 lists some example translations by VDBA vs Align-VDBA. We observe that VDBA places constraints at the end of the translated sentence (e.g., “pusher”, “develop-

ment”) unlike Align-VDBA. In some cases where constraints contain frequent words (like of, the, etc.), VDBA picks the token in the wrong position to tack on the constraint (e.g., “strong backing of”, “of qualified”) while Align-VDBA places the constraint correctly.

Dataset →	IATE.414		Wiktionary.727	
	BLEU (Δ)	CSR	BLEU (Δ)	CSR
Method (Beam Size) ↓				
Baseline (5)	25.8	76.3	26.0	76.9
Train-by-app. (5)	26.0 (+0.2)	92.9	26.9 (+0.9)	90.7
Train-by-rep. (5)	26.0 (+0.2)	94.5	26.3 (+0.3)	93.4
No constraints (10)	29.7	77.0	29.9	72.4
SHIFTAET (10)	29.9	95.9	30.4	97.2
VDBA (10)	30.9	99.8	30.9	99.4
Align-VDBA (10)	30.9 (+1.2)	99.8	31.1 (+1.2)	99.5

Table 5: Constrained translation results on the two real world constraints from Dinu et al. (2019).

Real World Constraints: We also evaluate on real world constraints extracted from IATE and Wiktionary datasets by Dinu et al. (2019). Table 5 compares Align-VDBA with the soft-constraints method of Dinu et al. (2019) that requires special retraining to teach the model to copy constraints. We reproduced the numbers from their paper in the first three rows. Their baseline is almost 4 BLEU points worse than ours since they used a smaller NMT model, thus making running times incomparable. When we compare the increment Δ in BLEU over the respective baselines, Align-VDBA shows

Constraints	(gesetz zur, law also), (dealer, pusher)
Gold	of course, if a drug addict becomes a pusher , then it is right and necessary that he should pay and answer before the law also .
VDBA	certainly, if a drug addict becomes a dealer , it is right and necessary that he should be brought to justice before the law also pusher .
Align-VDBA	certainly, if a drug addict becomes a pusher , then it is right and necessary that he should be brought to justice before the law also .
Constraints	(von mehrheitsverfahren, of qualified)
Gold	... whether this is done on the basis of a vote or of consensus, and whether unanimity is required or some form of of qualified majority.
VDBA	... whether this is done by means of of qualified votes or consensus, and whether unanimity or form of majority procedure apply.
Align-VDBA	... whether this is done by voting or consensus, and whether unanimity or form of of qualified majority voting are valid.
Constraints	(zustimmung der, strong backing of)
Gold	... which were adopted with the strong backing of the ppe group and the support of the socialist members.
VDBA	... which were then adopted with broad agreement of the ppe group and with the strong backing of the socialist members.
Align-VDBA	... which were then adopted with strong backing of the ppe group and with the support of the socialist members.
Constraints	(den usa, the usa), (sicherheitssystem an, security system that), (entwicklung, development)
Gold	matters we regard as particularly important are improving the working conditions between the weu and the eu and the development of a european security system that is not dependent on the usa .
VDBA	we consider the usa 's european security system to be particularly important in improving working conditions between the weu and the eu and developing a european security system that is independent of the united states development .
Align-VDBA	we consider the development of the security system that is independent of the usa to be particularly important in improving working conditions between the weu and the eu .

Table 4: Anecdotes showing constrained translations produced by VDBA vs. Align-VDBA.

much greater gains of +1.2 vs. their +0.5. Also, Align-VDBA provides a larger CSR of 99.6 compared to their 92. Results for other beam sizes and other methods and metrics appear in Appendix F.

5 Related Work

Online Prior Alignment from NMTs: Zenkel et al. (2019) find alignments using a single-head attention submodule, optimized to predict the next token. Garg et al. (2019) and Song et al. (2020) supervise a single alignment head from the penultimate multi-head attention with prior alignments from GIZA++ alignments or FastAlign. Bahar et al. (2020) and Shankar et al. (2018) treat alignment as a latent variable and impose a joint distribution over token and alignment while supervising on the token marginal of the joint distribution.

Online Posterior Alignment from NMTs: Shankar and Sarawagi (2019) first identify the role of posterior attention for more accurate alignment. However, their NMT was a single-headed RNN. Chen et al. (2020) implement posterior attention in a multi-headed Transformer but they incur a delay of one step between token output and alignment. We are not aware of any prior work that extracts truly online posterior alignment in modern NMTs.

Offline Alignment Systems: Several recent methods apply only in the offline setting: Zenkel et al. (2020) extend an NMT with an alignment module; Nagata et al. (2020) frame alignment as a question answering task; and Jalili Sabet et al. (2020); Dou and Neubig (2021) leverage contextual embeddings from pretrained multilingual models.

Lexicon Constrained Translation: Hokamp and Liu (2017) and Post and Vilar (2018); Hu et al.

(2019) modify beam search to ensure that target phrases from a given constrained lexicon are present in the translation. These methods ignore alignment with the source but ensure high success rate for appearance of the target phrases in the constraint. Song et al. (2020) and Chen et al. (2021) do consider source alignment but they do not enforce constraints leading to lower CSR. Dinu et al. (2019) and Lee et al. (2021) propose alternative training strategies for constraints, whereas we focus on working with existing models. Recently, non autoregressive methods have been proposed for enforcing target constraints but they require that the constraints are given in the order they appear in the target translation (Susanto et al., 2020).

6 Conclusion

In this paper we proposed a simple modification to NMT systems to obtain accurate online alignments. The key idea that led to high alignment accuracy was conditioning on the output token. Further, our alignment module enables such conditioning to be performed synchronously with token generation. This property led us to Align-VDBA, a principled decoding algorithm for lexically constrained translation based on joint distribution of target token and source alignments.

Limitations: All existing methods for hard constrained inference, including ours, come with considerable runtime overheads. Soft constrained methods are not accurate enough.

Future work: Future work could try to increase efficiency of constrained inference and handle other forms of constraints including nested constraints.

596
597
598
599
600
601
602
603

604
605
606
607
608
609
610

611
612
613
614
615
616

617
618
619
620
621

622
623
624
625
626

627
628
629
630
631
632

633
634
635
636
637
638
639

640
641
642
643
644
645
646
647
648
649
650

651
652

References

Tamer Alkhouli, Gabriel Bretschner, and Hermann Ney. 2018. [On the alignment problem in multi-head attention-based neural machine translation](#). In *Proceedings of the Third Conference on Machine Translation: Research Papers*, pages 177–185, Brussels, Belgium. Association for Computational Linguistics.

Parnia Bahar, Nikita Makarov, and Hermann Ney. 2020. [Investigation of transformer-based latent attention models for neural machine translation](#). In *Proceedings of the 14th Conference of the Association for Machine Translation in the Americas (Volume 1: Research Track)*, pages 7–20, Virtual. Association for Machine Translation in the Americas.

Dzmitry Bahdanau, Kyunghyun Cho, and Yoshua Bengio. 2015. [Neural machine translation by jointly learning to align and translate](#). In *3rd International Conference on Learning Representations, ICLR 2015, San Diego, CA, USA, May 7-9, 2015, Conference Track Proceedings*.

Peter F. Brown, Stephen A. Della Pietra, Vincent J. Della Pietra, and Robert L. Mercer. 1993. [The mathematics of statistical machine translation: Parameter estimation](#). *Computational Linguistics*, 19(2):263–311.

Guanhua Chen, Yun Chen, and Victor O.K. Li. 2021. [Lexically constrained neural machine translation with explicit alignment guidance](#). *Proceedings of the AAAI Conference on Artificial Intelligence*, 35(14):12630–12638.

Yun Chen, Yang Liu, Guanhua Chen, Xin Jiang, and Qun Liu. 2020. [Accurate word alignment induction from neural machine translation](#). In *Proceedings of the 2020 Conference on Empirical Methods in Natural Language Processing (EMNLP)*, pages 566–576, Online. Association for Computational Linguistics.

Kyunghyun Cho, Bart van Merriënboer, Dzmitry Bahdanau, and Yoshua Bengio. 2014. [On the properties of neural machine translation: Encoder–decoder approaches](#). In *Proceedings of SSST-8, Eighth Workshop on Syntax, Semantics and Structure in Statistical Translation*, pages 103–111, Doha, Qatar. Association for Computational Linguistics.

Josep Crego, Jungi Kim, Guillaume Klein, Anabel Rebollo, Kathy Yang, Jean Senellart, Egor Akhanov, Patrice Brunelle, Aurelien Coquard, Yongchao Deng, Satoshi Enoue, Chiyo Geiss, Joshua Johanson, Ardas Khalsa, Raoum Khiari, Byeongil Ko, Catherine Kobus, Jean Lorieux, Leidiana Martins, Dang-Chuan Nguyen, Alexandra Priori, Thomas Riccardi, Natalia Segal, Christophe Servan, Cyril Tiquet, Bo Wang, Jin Yang, Dakun Zhang, Jing Zhou, and Peter Zoldan. 2016. [Systran’s pure neural machine translation systems](#).

Shuoyang Ding, Hainan Xu, and Philipp Koehn. 2019. [Saliency-driven word alignment interpretation for](#)

[neural machine translation](#). In *Proceedings of the Fourth Conference on Machine Translation (Volume 1: Research Papers)*, pages 1–12, Florence, Italy. Association for Computational Linguistics. 653
654
655
656

Georgiana Dinu, Prashant Mathur, Marcello Federico, and Yaser Al-Onaizan. 2019. [Training neural machine translation to apply terminology constraints](#). In *Proceedings of the 57th Annual Meeting of the Association for Computational Linguistics*, pages 3063–3068, Florence, Italy. Association for Computational Linguistics. 657
658
659
660
661
662
663

Zi-Yi Dou and Graham Neubig. 2021. [Word alignment by fine-tuning embeddings on parallel corpora](#). In *Proceedings of the 16th Conference of the European Chapter of the Association for Computational Linguistics: Main Volume*, pages 2112–2128, Online. Association for Computational Linguistics. 664
665
666
667
668
669

Chris Dyer, Victor Chahuneau, and Noah A. Smith. 2013. [A simple, fast, and effective reparameterization of IBM model 2](#). In *Proceedings of the 2013 Conference of the North American Chapter of the Association for Computational Linguistics: Human Language Technologies*, pages 644–648, Atlanta, Georgia. Association for Computational Linguistics. 670
671
672
673
674
675
676
677

Sarthak Garg, Stephan Peitz, Udhayakumar Nallasamy, and Matthias Paulik. 2019. [Jointly learning to align and translate with transformer models](#). In *Proceedings of the 2019 Conference on Empirical Methods in Natural Language Processing and the 9th International Joint Conference on Natural Language Processing (EMNLP-IJCNLP)*, pages 4453–4462, Hong Kong, China. Association for Computational Linguistics. 678
679
680
681
682
683
684
685
686

Eva Hasler, Adrià de Gispert, Gonzalo Iglesias, and Bill Byrne. 2018. [Neural machine translation decoding with terminology constraints](#). In *Proceedings of the 2018 Conference of the North American Chapter of the Association for Computational Linguistics: Human Language Technologies, Volume 2 (Short Papers)*, pages 506–512, New Orleans, Louisiana. Association for Computational Linguistics. 687
688
689
690
691
692
693
694

Felix Hieber, Tobias Domhan, Michael Denkowski, and David Vilar. 2020. [Sockeye 2: A toolkit for neural machine translation](#). In *Proceedings of the 22nd Annual Conference of the European Association for Machine Translation*, pages 457–458, Lisboa, Portugal. European Association for Machine Translation. 695
696
697
698
699
700

Chris Hokamp and Qun Liu. 2017. [Lexically constrained decoding for sequence generation using grid beam search](#). In *Proceedings of the 55th Annual Meeting of the Association for Computational Linguistics (Volume 1: Long Papers)*, pages 1535–1546, Vancouver, Canada. Association for Computational Linguistics. 701
702
703
704
705
706
707

J. Edward Hu, Huda Khayrallah, Ryan Culkin, Patrick Xia, Tongfei Chen, Matt Post, and Benjamin

710	Van Durme. 2019. Improved lexically constrained decoding for translation and monolingual rewriting. In <i>Proceedings of the 2019 Conference of the North American Chapter of the Association for Computational Linguistics: Human Language Technologies, Volume 1 (Long and Short Papers)</i> , pages 839–850, Minneapolis, Minnesota. Association for Computational Linguistics.	
711		
712		
713		
714		
715		
716		
717		
718	Masoud Jalili Sabet, Philipp Dufter, François Yvon, and Hinrich Schütze. 2020. SimAlign: High quality word alignments without parallel training data using static and contextualized embeddings. In <i>Findings of the Association for Computational Linguistics: EMNLP 2020</i> , pages 1627–1643, Online. Association for Computational Linguistics.	
719		
720		
721		
722		
723		
724		
725	Nal Kalchbrenner and Phil Blunsom. 2013. Recurrent continuous translation models. In <i>Proceedings of the 2013 Conference on Empirical Methods in Natural Language Processing</i> , pages 1700–1709, Seattle, Washington, USA. Association for Computational Linguistics.	
726		
727		
728		
729		
730		
731	Philipp Koehn, Amittai Axelrod, Alexandra Birch Mayne, Chris Callison-Burch, Miles Osborne, and David Talbot. 2005. Edinburgh system description for the 2005 iwslt speech translation evaluation. In <i>International Workshop on Spoken Language Translation (IWSLT) 2005</i> .	
732		
733		
734		
735		
736		
737	Anoop Kunchukuttan, Pratik Mehta, and Pushpak Bhat-tacharyya. 2018. The IIT Bombay English-Hindi parallel corpus. In <i>Proceedings of the Eleventh International Conference on Language Resources and Evaluation (LREC 2018)</i> , Miyazaki, Japan. European Language Resources Association (ELRA).	
738		
739		
740		
741		
742		
743	Gyubok Lee, Seongjun Yang, and Edward Choi. 2021. Improving lexically constrained neural machine translation with source-conditioned masked span prediction. In <i>Proceedings of the 59th Annual Meeting of the Association for Computational Linguistics and the 11th International Joint Conference on Natural Language Processing (Volume 2: Short Papers)</i> , pages 743–753, Online. Association for Computational Linguistics.	
744		
745		
746		
747		
748		
749		
750		
751		
752	Joel Martin, Rada Mihalcea, and Ted Pedersen. 2005. Word alignment for languages with scarce resources. In <i>Proceedings of the ACL Workshop on Building and Using Parallel Texts</i> , pages 65–74, Ann Arbor, Michigan. Association for Computational Linguistics.	
753		
754		
755		
756		
757		
758	Rada Mihalcea and Ted Pedersen. 2003. An evaluation exercise for word alignment. In <i>Proceedings of the HLT-NAACL 2003 Workshop on Building and Using Parallel Texts: Data Driven Machine Translation and Beyond</i> , pages 1–10.	
759		
760		
761		
762		
763	Mathias Müller. 2017. Treatment of markup in statistical machine translation. In <i>Proceedings of the Third Workshop on Discourse in Machine Translation</i> , pages 36–46, Copenhagen, Denmark. Association for Computational Linguistics.	
764		
765		
766		
767		
	Masaaki Nagata, Katsuki Chousa, and Masaaki Nishino. 2020. A supervised word alignment method based on cross-language span prediction using multilingual BERT. In <i>Proceedings of the 2020 Conference on Empirical Methods in Natural Language Processing (EMNLP)</i> , pages 555–565, Online. Association for Computational Linguistics.	768 769 770 771 772 773 774
	Graham Neubig. 2011. The Kyoto free translation task.	775
	Franz Josef Och and Hermann Ney. 2000. Improved statistical alignment models. In <i>Proceedings of the 38th Annual Meeting of the Association for Computational Linguistics</i> , pages 440–447, Hong Kong. Association for Computational Linguistics.	776 777 778 779 780
	Franz Josef Och and Hermann Ney. 2003. A systematic comparison of various statistical alignment models. <i>Computational Linguistics</i> , 29(1):19–51.	781 782 783
	Myle Ott, Sergey Edunov, Alexei Baevski, Angela Fan, Sam Gross, Nathan Ng, David Grangier, and Michael Auli. 2019. fairseq: A fast, extensible toolkit for sequence modeling. In <i>Proceedings of the 2019 Conference of the North American Chapter of the Association for Computational Linguistics (Demonstrations)</i> , pages 48–53, Minneapolis, Minnesota. Association for Computational Linguistics.	784 785 786 787 788 789 790 791
	Kishore Papineni, Salim Roukos, Todd Ward, and Wei-Jing Zhu. 2002. Bleu: a method for automatic evaluation of machine translation. In <i>Proceedings of the 40th Annual Meeting of the Association for Computational Linguistics</i> , pages 311–318, Philadelphia, Pennsylvania, USA. Association for Computational Linguistics.	792 793 794 795 796 797 798
	Matt Post. 2018. A call for clarity in reporting BLEU scores. In <i>Proceedings of the Third Conference on Machine Translation: Research Papers</i> , pages 186–191, Brussels, Belgium. Association for Computational Linguistics.	799 800 801 802 803
	Matt Post and David Vilar. 2018. Fast lexically constrained decoding with dynamic beam allocation for neural machine translation. In <i>Proceedings of the 2018 Conference of the North American Chapter of the Association for Computational Linguistics: Human Language Technologies, Volume 1 (Long Papers)</i> , pages 1314–1324, New Orleans, Louisiana. Association for Computational Linguistics.	804 805 806 807 808 809 810 811
	Rico Sennrich, Barry Haddow, and Alexandra Birch. 2016. Neural machine translation of rare words with subword units. In <i>Proceedings of the 54th Annual Meeting of the Association for Computational Linguistics (Volume 1: Long Papers)</i> , pages 1715–1725, Berlin, Germany. Association for Computational Linguistics.	812 813 814 815 816 817 818
	Shiv Shankar, Siddhant Garg, and Sunita Sarawagi. 2018. Surprisingly easy hard-attention for sequence to sequence learning. In <i>Proceedings of the 2018 Conference on Empirical Methods in Natural Language Processing</i> , pages 640–645, Brussels, Belgium. Association for Computational Linguistics.	819 820 821 822 823 824

825 Shiv Shankar and Sunita Sarawagi. 2019. [Posterior at-](#)
826 [tention models for sequence to sequence learning.](#)
827 *In International Conference on Learning Representations.*
828

829 Xiaoyu Shen, Yang Zhao, Hui Su, and Dietrich Klakow.
830 2019. [Improving latent alignment in text summa-](#)
831 [rization by generalizing the pointer generator.](#) *In*
832 *Proceedings of the 2019 Conference on Empirical*
833 *Methods in Natural Language Processing and the*
834 *9th International Joint Conference on Natural Lan-*
835 *guage Processing (EMNLP-IJCNLP)*, pages 3762–
836 3773, Hong Kong, China. Association for Computa-
837 tional Linguistics.

838 Kai Song, Kun Wang, Heng Yu, Yue Zhang,
839 Zhongqiang Huang, Weihua Luo, Xiangyu Duan,
840 and Min Zhang. 2020. [Alignment-enhanced trans-](#)
841 [former for constraining nmt with pre-specified trans-](#)
842 [lations.](#) *Proceedings of the AAAI Conference on Ar-*
843 *tificial Intelligence*, 34(05):8886–8893.

844 Raymond Hendy Susanto, Shamil Chollampatt, and
845 Liling Tan. 2020. [Lexically constrained neural ma-](#)
846 [chine translation with Levenshtein transformer.](#) *In*
847 *Proceedings of the 58th Annual Meeting of the Asso-*
848 *ciation for Computational Linguistics*, pages 3536–
849 3543, Online. Association for Computational Lin-
850 guistics.

851 Ilya Sutskever, Oriol Vinyals, and Quoc V Le. 2014.
852 [Sequence to sequence learning with neural networks.](#)
853 *In Advances in Neural Information Processing Sys-*
854 *tems*, volume 27. Curran Associates, Inc.

855 Ashish Vaswani, Noam Shazeer, Niki Parmar, Jakob
856 Uszkoreit, Llion Jones, Aidan N Gomez, Łukasz
857 Kaiser, and Illia Polosukhin. 2017. [Attention is all](#)
858 [you need.](#) *In Advances in Neural Information Pro-*
859 *cessing Systems*, volume 30. Curran Associates, Inc.

860 David Vilar, Maja Popović, and Hermann Ney. 2006.
861 [AER: Do we need to “improve” our alignments?](#) *In*
862 *International Workshop on Spoken Language Trans-*
863 *lation (IWSLT) 2006.*

864 Thomas Zenkel, Joern Wuebker, and John DeNero.
865 2019. [Adding interpretable attention to neural trans-](#)
866 [lation models improves word alignment.](#)

867 Thomas Zenkel, Joern Wuebker, and John DeNero.
868 2020. [End-to-end neural word alignment outper-](#)
869 [forms GIZA++.](#) *In Proceedings of the 58th Annual*
870 *Meeting of the Association for Computational Lin-*
871 *guistics*, pages 1605–1617, Online. Association for
872 Computational Linguistics.

A Alignment Error Rate

Given gold alignments consisting of sure alignments \mathcal{S} and possible alignments \mathcal{P} , and the predicted alignments \mathcal{A} , the Alignment Error Rate (AER) is defined as (Och and Ney, 2000):

$$\text{AER} = 1 - \frac{|\mathcal{A} \cap \mathcal{P}| + |\mathcal{A} \cap \mathcal{S}|}{|\mathcal{A}| + |\mathcal{S}|}$$

Note that here $\mathcal{S} \subseteq \mathcal{P}$. Also note that since our models are trained on sub-word units but gold alignments are over words, we need to convert alignments between word pieces to alignments between words. A source word and target word are said to be aligned if there exists an alignment link between any of their respective word pieces.

B BLEU-C

Given a reference sentence, a predicted translation and a set of constraints, for each constraints, a segment of the sentence is chosen which contains the constraint and window size words (if available) surrounding the constraint words on either side. Such segments, called spans, are collected for the reference and predicted sentences in the test and BLEU is computed over these spans. If a constraint is not satisfied in the prediction, the corresponding span is considered to be the empty string. An example is shown in Table 6. Table 7 shows how BLEU-C varies as a function of varying window size for a fixed English-French constraint set with beam size set to 10.

Window Size \rightarrow	2	3	4	5	6	7	8
No constraints	0.0	0.0	0.0	0.0	0.0	0.0	0.0
NAIVEATT	34.4	32.0	30.4	29.5	29.4	29.5	29.7
PRIORATT	41.5	38.7	36.4	35.1	34.9	35.0	35.2
SHIFTATT	44.9	41.5	38.9	37.3	36.4	36.2	36.0
SHIFTAET	47.0	43.2	40.4	38.7	38.0	37.6	37.4
POSTALN	46.4	42.7	39.8	38.0	37.1	36.9	36.6
VDBA	54.9	50.5	46.8	44.6	43.5	43.0	42.6
Align-VDBA	56.4	51.7	47.9	45.6	44.4	43.7	43.3

Table 7: BLEU-C vs Window Size

C Description of the Datasets

The European languages consist of parallel sentences for three language pairs from the Europarl Corpus and alignments from Mihalcea and Pedersen (2003), Och and Ney (2000), Vilar et al. (2006). Following previous works (Ding et al., 2019; Chen et al., 2020), the last 1000 sentences of the training data are used as validation data.

For English-Hindi, we use the dataset from Martin et al. (2005) consisting of 3440 training sentence

pairs, 25 validation and 90 test sentences with gold alignments. Since training Transformers requires much larger datasets, we augment the training set with 1.6 million sentences from the IIT Bombay Parallel Corpus (Kunchukuttan et al., 2018). We also add the first 50 sentences from the dev set of IIT Bombay Parallel Corpus with manually annotated alignments to the test set giving a total of 140 test sentences.

For Japanese-English, we use The Kyoto Free Translation Task (Neubig, 2011). It comprises roughly 330K training, 1166 validation and 1235 test sentences. As with other datasets, gold alignments are available only for the test sentences. The Japanese text is already segmented and we use it without additional changes.

The real world constraints datasets of Dinu et al. (2019) are extracted from the German-English WMT newstest 2017 task with the IATE dataset consisting of 414 sentences (451 constraints) and the Wiktionary 727 sentences (879 constraints). The constraints come from the IATE and Wiktionary terminology databases.

All datasets were processed using the scripts provided by Zenkel et al. (2019) at <https://github.com/lilt/alignment-scripts>. Computation of BLEU and BLEU-C, and the paired test were performed using sacrebleu (Post, 2018).

D Bidirectional Symmetrized Alignment

We report AERs using bidirectional symmetrized alignments in Table 8 in order to provide fair comparisons to results in prior literature. The symmetrization is done using the *grow-diagonal* heuristic (Koehn et al., 2005; Och and Ney, 2000). Since bidirectional alignments need the entire text in both languages, these are not online alignments.

Method	de-en	en-fr	ro-en	en-hi	ja-en
Statistical Methods					
GIZA++	18.6	5.5	26.3	35.9	39.7
FastAlign	27.0	10.5	32.1	-	-
No Alignment Training					
NAIVEATT	29.2	16.9	31.4	43.8	57.1
SHIFTATT	16.9	7.8	24.3	30.9	46.2
With Alignment Training					
PRIORATT	22.0	10.1	26.3	32.1	48.2
SHIFTAET	15.4	5.6	21.0	26.7	40.1
POSTALN	15.3	5.5	21.0	26.1	39.5

Table 8: AERs for bidirectional symmetrized alignments. POSTALN consistently performs the best.

Reference	we consider the development of a robust security system that is independent of the	
Prediction	we consider developing a robust security system which is independent of the	
BLEU-C (Window Size = 2)		
Cons. No	Reference Spans	Predicted Spans
1	consider the development of a	(empty sentence)
2	a robust security system that is	a robust security system which is
BLEU-C = BLEU(Reference Spans, Predicted Spans)		

Table 6: An example BLEU-C computation

E Additional Lexicon-Constrained Translation Results

Constrained translation results for beam sizes 5 and 10 are shown in Table 9. Paired bootstrap resampling test results with respect to Align-VDBA for beam size 10 are shown in Table 10.

F Additional Real World Constrained Translation Results

Results on the real world constrained translation datasets of Dinu et al. (2019) for all the methods in Table 3 with beam sizes 5, 10 and 20 are presented in Table 11. Paired bootstrap resampling test results with respect to Align-VDBA for beam size 5 are shown in Table 12

G Alignment-based Token Replacement Algorithm

The pseudocode for the algorithm used in Song et al. (2020); Chen et al. (2021) and our non-VDBA based methods in Section 4.3 is presented in Algorithm 2. As described in Section 3.1, at each decoding step, if the source token having the maximum alignment at the current step lies in some constraint span, the constraint in question is decoded until completion before resuming normal decoding.

Though different alignment methods are represented using a call to the same ATTENTION function in Algorithm 2, these methods incur varying computational overheads. For instance, NAIVEATT incurs little additional cost, PRIORATT and POSTALN involve a multi-head attention computation. For SHIFTATT and SHIFTAET, an entire decoder pass is done when ATTENTION is called, thereby incurring a huge overhead as shown in Table 3.

H Layer Selection for Alignment Supervision of Distant Language Pairs

For the alignment supervision, we used alignments extracted from vanilla Transformers using the SHIFTATT method. To do so, however, we need to choose the decoder layers from which to extract the alignments. The validation AERs can be used for this purpose but since gold validation alignments are not available, Chen et al. (2020) suggest selecting the layers which have the best consistency between the alignment predictions from the two translation directions.

For the European language pairs, this turns out to be layer 3 as suggested by Chen et al. (2020). However, for the distant language pairs Hindi-English and Japanese-English, this is not the case and layer selection needs to be done. The AER between the two translation directions on the validation set, with alignments obtained from different decoder layers, are shown in Tables 13 and 14.

948
949

950
951
952
953

954
955

956
957
958
959
960
961

962
963

964
965
966
967
968
969
970
971
972

973
974
975
976
977
978
979
980
981
982

983
984

985
986
987
988
989
990
991
992
993
994
995
996
997
998
999
1000
1001
1002

Beam Size	Method	de→en				en→fr				ro→en				en→hi				ja→en			
		BLEU-C	CSR	BLEU	Time	BLEU-C	CSR	BLEU	Time	BLEU-C	CSR	BLEU	Time	BLEU-C	CSR	BLEU	Time	BLEU-C	CSR	BLEU	Time
5	No constraints	0.0	5.0	32.9	78	0.0	8.7	34.6	61	0.0	8.4	33.3	45	0.0	5.6	19.7	18	0.0	7.9	19.1	221
	NAIVEATT	28.9	86.2	36.7	127	36.7	88.6	38.0	87	32.9	91.8	36.3	88	23.0	89.9	23.9	25	15.1	77.0	20.3	398
	PRIORATT	35.3	93.0	37.7	136	42.2	94.7	38.6	89	36.0	91.6	37.0	89	27.6	91.7	24.7	26	16.8	80.2	20.6	353
	SHIFTATT	41.0	96.7	38.7	268	45.2	93.8	38.4	167	39.2	94.4	37.2	160	23.8	81.8	22.0	42	15.1	72.6	19.3	664
	SHIFTAET	43.1	97.6	39.1	291	46.5	94.8	38.6	165	40.8	94.7	37.5	163	24.5	83.6	22.1	44	18.0	76.5	19.6	583
	POSTALN	42.7	97.3	39.0	252	46.1	93.9	38.5	151	39.8	93.5	37.3	141	23.3	79.7	21.7	39	17.9	75.3	19.6	469
	VDBA	39.6	99.4	37.8	203	45.9	99.5	38.5	109	36.6	99.2	36.7	117	27.3	96.6	24.2	37	22.1	96.9	20.9	397
	Align-VDBA	41.3	98.8	38.2	236	48.0	98.9	38.7	128	42.0	96.6	37.5	134	28.2	91.3	24.7	45	22.6	93.9	21.2	445
10	No constraints	0.0	4.6	32.9	87	0.0	8.7	34.8	64	0.0	8.8	33.4	47	0.0	6.3	19.7	21	0.0	8.8	18.9	237
	NAIVEATT	28.7	86.1	36.6	147	36.5	88.0	38.3	93	33.3	92.3	36.5	99	22.5	88.4	23.6	27	15.1	75.9	20.2	315
	PRIORATT	35.0	92.8	37.6	159	42.1	94.4	38.9	97	36.0	91.2	37.2	100	27.2	91.5	24.4	28	16.7	79.7	20.4	326
	SHIFTATT	41.0	96.6	38.7	443	45.0	93.5	38.7	239	39.2	94.2	37.4	241	23.2	78.7	21.9	58	15.2	72.7	19.3	567
	SHIFTAET	43.1	97.5	39.1	458	46.6	94.3	39.0	235	40.8	94.4	37.6	263	24.3	80.2	22.0	62	18.1	75.9	19.7	596
	POSTALN	42.7	97.2	39.0	399	46.3	94.1	38.7	218	41.0	93.5	37.4	226	23.8	79.0	22.0	47	18.2	75.7	19.7	460
	VDBA	44.5	98.9	38.5	293	51.9	98.5	39.5	160	43.1	99.1	37.9	165	29.8	92.3	24.5	49	24.3	95.6	21.6	494
	Align-VDBA	44.5	98.6	38.6	357	52.9	98.4	39.7	189	44.1	98.9	38.1	203	30.5	91.5	24.7	70	25.1	95.5	21.8	630

Table 9: Lexically Constrained Translation Results with different beam sizes. All numbers are average over 5 randomly sampled constraint sets and running times are in seconds.

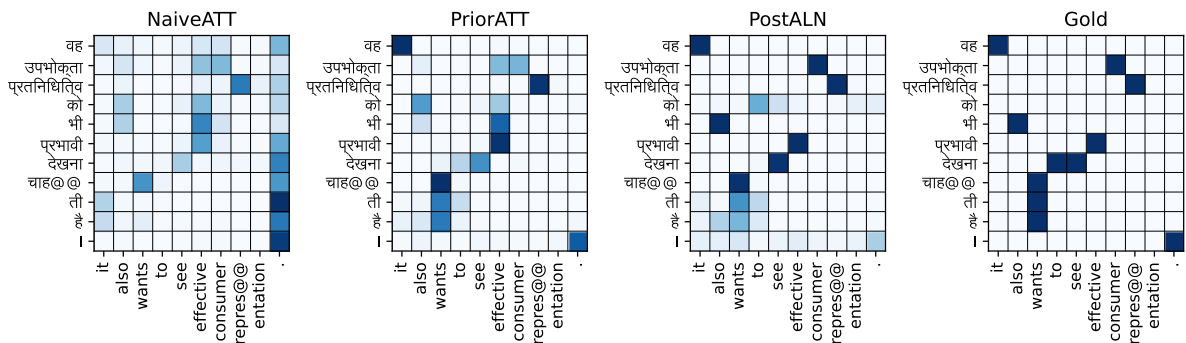


Figure 3: Alignments for en→hi by NAIVEATT, PRIORATT, and POSTALN. Note that POSTALN is most similar to Gold alignments in the last column.

	de→en	en→fr	ro→en
No constraints	0.0001*	0.0001*	0.0001*
NAIVEATT	0.0001*	0.0001*	0.0001*
PRIORATT	0.0001*	0.0001*	0.0001*
SHIFTATT	0.1700	0.0001*	0.0001*
SHIFTAET	0.0015*	0.0001*	0.0018*
POSTALN	0.0032*	0.0001*	0.0003*
VDBA	0.2666	0.0020*	0.0229*

Table 10: Paired bootstrap resampling tests with 10000 bootstrap samples for BLEU on Table 3 datasets for beam size 10. * denotes statistically significant difference from Align-VDBA at power 0.05 (p-value < 0.05).

Beam Size	Dataset →	IATE.414				Wiktionary.727				
		Method ↓	BLEU-C	CSR	BLEU	Time	BLEU-C	CSR	BLEU	Time
5	No constraints		27.9	76.6	29.7	134	26.3	72.0	29.9	217
	NAIVEATT		29.2	96.9	29.2	175	29.0	95.3	29.1	341
	PRIORATT		31.2	97.1	29.7	198	32.2	95.9	29.9	306
	SHIFTATT		34.9	96.7	29.9	355	35.3	96.5	30.0	568
	SHIFTAET		35.2	96.3	30.0	378	35.8	97.1	30.2	637
	POSTALN		35.3	96.7	30.0	272	35.8	96.7	30.2	467
	VDBA		35.3	98.8	29.8	258	35.0	99.2	30.4	442
	Align-VDBA		36.1	98.3	30.1	268	35.9	98.8	30.6	523
10	No constraints		28.3	77.0	29.7	113	26.3	72.4	29.9	164
	NAIVEATT		28.9	97.3	29.1	145	29.2	95.3	29.1	269
	PRIORATT		31.3	96.9	29.5	155	32.3	96.0	29.9	260
	SHIFTATT		34.9	96.3	29.8	345	35.3	96.8	30.3	600
	SHIFTAET		35.2	95.9	29.9	350	35.9	97.2	30.4	664
	POSTALN		35.1	95.9	29.9	287	35.8	97.0	30.3	458
	VDBA		37.6	99.8	30.9	257	36.9	99.4	30.9	451
	Align-VDBA		37.5	99.8	30.9	353	37.2	99.5	31.1	540
20	No constraints		28.4	77.2	29.9	103	26.3	72.1	30.0	177
	NAIVEATT		28.9	96.9	29.0	188	29.1	95.4	29.3	325
	PRIORATT		31.3	96.9	29.6	203	32.6	96.4	30.1	338
	SHIFTATT		34.7	96.1	29.8	528	35.3	96.8	30.2	892
	SHIFTAET		35.0	95.8	29.9	539	36.1	97.3	30.4	923
	POSTALN		35.1	96.1	29.9	420	36.0	97.0	30.4	751
	VDBA		37.8	99.8	30.9	381	37.4	99.2	31.2	680
	Align-VDBA		37.9	99.8	30.9	465	38.0	99.5	31.3	818

Table 11: Additional results for the real world constraints for all methods and different beam sizes.

Algorithm 2 k -best extraction with argmax replacement decoding.

Inputs: A $k \times |V_T|$ matrix of scores (for all tokens up to the currently decoded ones). k beam states.

```
1: function SEARCH_STEP(beam, scores)
2:   next_toks, next_scores  $\leftarrow$  ARGMAX_K(scores, k=2, dim=1)  $\triangleright$  Best 2 tokens for each beam
3:   candidates  $\leftarrow$  []
4:   for  $0 \leq h < 2 \cdot k$  do
5:     candidate  $\leftarrow$  beam[h//2]
6:     candidate.tokens.append(next_toks[h//2, h%2])
7:     candidate.scores  $\leftarrow$  next_scores[h//2, h%2]
8:     candidates.append(candidate)
9:   attention  $\leftarrow$  ATTENTION(candidates)
10:  aligned_x  $\leftarrow$  ARGMAX(attention, dim=1)
11:  for  $0 \leq h < 2 \cdot k$  do
12:    if aligned_x[h]  $\in C_i^x$  for some  $i$  and not candidates[h].inprogress then  $\triangleright$  Start constraint
13:      candidates[h].inprogress  $\leftarrow$  True
14:      candidates[h].constraintNum  $\leftarrow i$ 
15:      candidates[h].tokenNum  $\leftarrow 0$ 
16:    if candidates[h].inprogress then  $\triangleright$  Replace token with constraint tokens
17:      candidates[h].tokens[-1]  $\leftarrow$  constraints[candidates[h].constraintNum][candidates[h].tokenNum]
18:      candidates[h].tokenNum  $\leftarrow$  candidates[h].tokenNum + 1
19:    if constraints[candidates[h].constraintNum].length == candidates[h].tokenNum then
20:      candidates[h].inprogress  $\leftarrow$  False  $\triangleright$  Finish current constraint
21:  candidates  $\leftarrow$  REMOVE_DUPLICATES(candidates)
22:  newBeam  $\leftarrow$  TOP_K(candidates)
23:  return newBeam
```

Dataset	IATE.414			Wiktionary.727		
	BLEU	$\mu \pm 95\%$ CI	p-value	BLEU	$\mu \pm 95\%$ CI	p-value
Align-VDBA	30.1	(30.0 \pm 1.7)		30.6	(30.6 \pm 1.2)	
No constraints	29.7	(29.7 \pm 1.7)	0.1059	29.9	(29.9 \pm 1.2)	0.0054*
NAIVEATT	29.2	(29.2 \pm 1.7)	0.0121*	29.1	(29.1 \pm 1.2)	0.0001*
PRIORATT	29.7	(29.6 \pm 1.6)	0.0829	29.9	(29.8 \pm 1.2)	0.0041*
SHIFTATT	29.9	(29.8 \pm 1.6)	0.1827	30.0	(30.0 \pm 1.2)	0.0229*
SHIFTAET	30.0	(29.9 \pm 1.6)	0.2824	30.2	(30.2 \pm 1.2)	0.0588
POSTALN	30.0	(30.0 \pm 1.6)	0.3813	30.2	(30.2 \pm 1.2)	0.0646
VDBA	29.8	(29.7 \pm 1.6)	0.0849	30.4	(30.4 \pm 1.2)	0.0960

Table 12: Paired bootstrap resampling tests with 10000 bootstrap samples for BLEU on [Dinu et al. \(2019\)](#) datasets for beam size 5. * denotes statistically significant difference from Align-VDBA at power 0.05 (p-value < 0.05).

	1	2	3	4	5	6
1	65.5	55.8	56.1	95.2	94.6	96.6
2	59.2	47.5	44.5	95.1	91.9	95.8
3	62.6	52.1	48.3	93.7	91.4	95.2
4	88.6	83.3	82.1	89.9	88.0	90.3
5	91.6	87.7	88.5	91.4	88.8	90.2
6	93.5	91.1	92.5	92.5	90.5	90.7

Table 13: AER between en→hi and hi→en SHIF-TATT alignments on the validation set for EnHi

	1	2	3	4	5	6
1	93.5	90.0	94.4	92.2	95.1	95.1
2	86.5	58.7	86.9	69.4	87.2	86.2
3	87.4	59.4	87.1	69.1	87.1	86.2
4	89.1	69.1	85.9	74.2	84.9	85.4
5	93.4	88.5	89.1	87.1	86.8	88.1
6	93.5	89.4	90.0	88.1	87.7	88.7

Table 14: AER between ja→en and en→ja SHIF-TATT alignments on the validation set for JaEn